ELSEVIER

www.elsevier.nl/locate/ica

Inorganica Chimica Acta 313 (2001) 125–136

Inorganica Chimica Acta

# Phosphoester hydrolysis using structural phosphatase models of tren based zinc(II) complexes and X-ray crystal structures of $[Zn(tren)(H_2O)](ClO_4)_2$ and $[Zn(tren)(BNPP)]ClO_4$

M.M. Ibrahim [a], Noriyuki Shimomura [a], Kazuhiko Ichikawa [a,*], Motoo Shiro [b]

[a] *Division of Material Science, Graduate School of Environmental Earth Science, Hokkaido University, Sapporo 060-0810, Japan*
[b] *X-ray Research Laboratory, Rigaku Corporation, Akishima 196-8666, Japan*

Received 22 July 2000; accepted 8 November 2000

**Abstract**

New tris(2-aminoethyl)amine (tren) L1 based ligands, namely *N*,*N*′,*N*″-tris(2-benzylaminoethyl)amine L2 and *N*,*N*′,*N*″-tris(im-benzyl-L-histidylethylaminoethyl) amine L3 have been synthesized and characterized. Complexation studies on $Zn^{2+}$ complexes **1**, **2** and **3** derived from L1, L2, and L3 showed that the presence of benzyl and benzyl–histidyl moieties attached to the tripodal ligand L1 side arms decrease the $pK_a$ of the Zn-bound water molecule: 10.72 for **1**, 9.61 for **2** and 7.43 for **3**, respectively. The zinc complex of **3** was a much more active catalyst for the hydrolysis of bis(*p*-nitrophenyl)phosphate ($BNPP^-$) and tris(*p*-nitrophenyl)phosphate (TNPP) compared with **1** and **2**. In the case of **1** and **2**, the pH-dependence of their observed pseudo-first-order rate constants $k_{obsd}$ showed sigmoidal pH–rate profile, while **3** gave bell-shape curve with a maximum rate constant of around $1.0 \times 10^{-5}$ $s^{-1}$ at pH 8.5. The pH dependence of $k_{obsd}$ indicated that the Zn-bound hydroxo species is responsible for catalytic activity. The crystal structures of $[L1Zn–H_2O]^{2+}$ (**1**) and $[L1Zn–BNPP]^+$ (**4**) have been determined and showed trigonal–bipyramidal configurations around the central Zn. The zinc complexes of **1** and **4** served as structural models for the binding mode of coordinated water as well as substrates in the active site of zinc enzyme. 

*Keywords:* Syntheses; Crystal structures; Stability constants; Deprotonation constants; Zinc complex catalysis; Phosphate ester hydrolysis

## 1. Introduction

Reaction mechanisms of hydrolytic zinc enzymes (e.g. alkaline phosphatase (AP)) and the role of the zinc ions in its active centers have constantly been interesting bioinorganic subjects [1]. These zinc enzymes often use external water molecules or internal alcoholic residues as nucleophiles to react with electrophilic substrates, wherein the prior activation of the nucleophile is essential [2]. The primary catalytic step is to produce a phosphorylserine intermediate that is subsequently hydrolyzed [3]. This latter step requires that $H_2O$ in the active site of AP be activated to the point that it can cleave nucleophilically a normally unreactive phosphate [4]. In turn, this ability seems to arise from the imposition of a fairly hydrophobic micro-environment, a lower coordination number than that adapted in bulk water and an efficient proton shuttling mechanism [5]. It has been postulated that the local hydrophobic environment in the proximity of zinc-bound water tends to decrease the $pK_a$ of the coordinated water molecule [6].

Recently, in order to mimic the zinc(II) coordination structure as well as the function of the zinc(II) ion at the active site, several mononuclear zinc(II) complexes have been designed and investigated to elucidate the detailed reaction mechanism in these zinc enzymes [7].

Although most hydrolytic enzymes contain Zn(II) and histidine imidazole which forms a tetrahedral coordination environment [8], most model complexes are not similar in structure to that of hydrolytic enzymes. Therefore, tripod-like ligands with a variety of ligating groups which tend to form a tetrahedron or trigonal bipyramids are of great interest [9]. However, the synthesis of imidazole containing tripodal ligands is tedious and only few papers have appeared recently [10].

* Corresponding author. Fax: +81-11-706 4528.
*E-mail address:* ichikawa@ees.hokudai.ac.jp (K. Ichikawa).

0020-1693/01/$ - see front matter 
PII: S0020-1693(00)00381-9

The mechanism of the cleavage of the phosphoester bond requires the active participation of one or more metal-coordinated water/hydroxide ion. In most cases only indirect evidence (e.g. pH–titration, pH–rate profile correlation) can prove its existence. There are very few crystal structures of model complexes with metal-coordinated water molecules present in available literature, and zinc containing models are especially rare. So there is a strong need to demonstrate directly the presence of water coordinated to the central metal ion(s) in catalytically active model complexes.

Tris(2-aminoethyl)amine, L1 is a well known and widely studied tripodal amine containing four coordination sites. Its ability of complex formation with zinc ion has been studied but mostly from the coordination-chemical point of view [11].

Our aim is to synthesize two new tripodal ligands *N*,*N*′,*N*″-tris(2-benzylaminoethyl) amine, L2 and *N*,*N*′,*N*″ - tris(im - benzyl - L - histidylethylaminoethyl) amine, L3 (Scheme 1) by affixing different coordination sites with bulky substituents on the periphery of tris(2-aminoethyl)amine, L1 on the assumption that upon complexation of Zn(II) ion, calix-like structures can be obtained and the environment around coordinated water molecules can be changed from hydrophilic to hydrophobic. The catalytic hydrolyses of bis(*p*-nitrophenyl)phosphate ($BNPP^-$) and tris(*p*-nitrophenyl)phosphate (TNPP) by designed mono-nuclear zinc complexes **1**, **2** and **3** derived from L1, L2, and L3, respectively, have been studied in the light of the possible effects of the hydrophobic groups on the acid dissociation constants of Zn(II)-bound water molecule. The crystal structures of L1–Zn(II) complexes with coordinated water $[L1Zn–H_2O]^{2+}$ (**1**) and coordinated phosphate $[L1Zn–BNPP]^+$ (**4**) were also obtained.

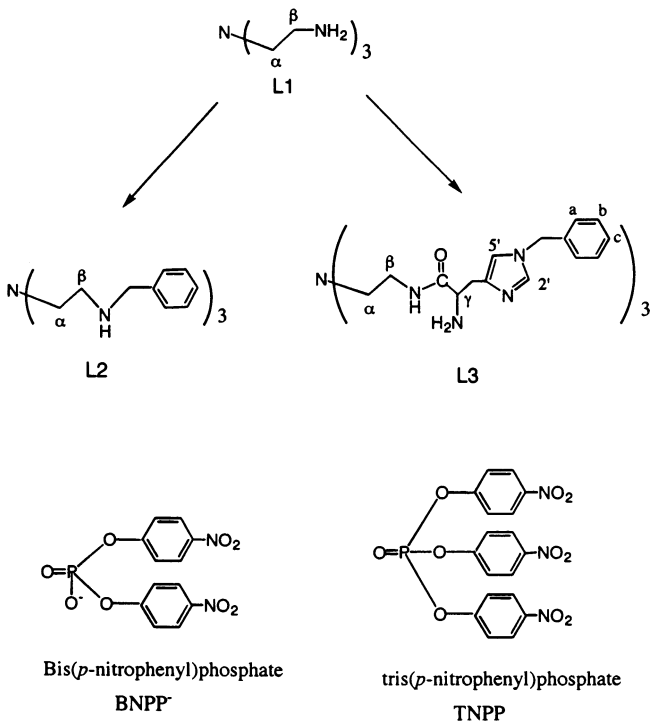


Scheme 1.

## 2. Experimental

### 2.1. Materials

All reagents and solvents used were of analytical grade. *N*(α)-*t*-butoxycarbonyl-*N*-(π)-benzyl-L-histidine [*N*(α)-Boc-im-bzl-L-His-OH] was purchased from Sigma. bis(4-Nitrophenyl)phosphate ($BNPP^-$), tris(4-nitrophenyl)phosphate (TNPP), tris(2-aminoethyl)-amine (L1) were taken from Tokyo Kasei Organic Chemical Company. Benzaldehyde was from Nacalai. Other chemicals were purchased from Wako. Anion-exchange resin 1- × 8, 100–200 mesh, Cl form was from Muromachi Kagaku Kogyo Kaisha Ltd.

*Caution:* perchlorate salts of amine ligands and their metal complexes are potentially explosive and should be handled in small quantities.

### 2.2. Synthesis

The synthesis of L2 was neatly performed by condensation of tris(2-aminoethyl)amine (tren) L1 with three equivalents of benzaldehyde and subsequent reduction of the imine with $NaBH_4$. Ligand L3 was synthesized by the reaction between L1 and *N*(α)-*t*-butoxycarbonyl-*N*-(π)-benzyl-L-histidine ((*N*(α)-Boc-im-bzl-L-His-OH) using the conventional solution phase method by using the racemization free and fragment condensation strategies. Zinc complexes of **1**, **2** and **3** were prepared by the reaction of the corresponding ligands with equimolar amounts of $Zn(ClO_4)_2$ in methanol.

#### 2.2.1. *N*,*N*′,*N*″-tris[(2-benzylamino)ethyl]amine L2

Tris(2-aminoethyl)amine L1 (0.512 ml, 3.42 mmol) and benzaldehyde (1.04 ml, 10.26 mmol) were dissolved in methanol (20 ml) and vigorously stirred at room temperature (r.t.) and refluxed for 2 h. A white precipitate was formed on cooling, filtered off, washed out with methanol, and dried in vacuo. $^1H$ NMR showed the disappearance of the aldehyde singlet and appearance of a new imine signal at 8.1 ppm. The tris–imine derivative was then added to a solution of 500 mg (13.2 mmol) of $NaBH_4$ in methanol and the reaction was let to stir overnight at r.t. The resultant solution was acidified by concentrated $HClO_4$. White precipitate of $L2{\cdot}3HClO_4$ was formed, filtered, and dried up: Found: C, 43.18; H, 5.73; Cl, 14.06; N, 7.41. *Anal.* Calc. for $C_{27}H_{36}N_4{\cdot}3HClO_4{\cdot}2H_2O$: C, 43.22; H, 5.76; Cl, 14.12; N, 7.43%. $^1H$ NMR ($D_2O$) 7.51–7.45 (m, 15H, $C_6H_5$–),

4.22 (s, 6H, Ph–C$H_2$–), and 2.87–2.82 ppm (t, 12H, N–$^{\alpha}$C$H_2$–$^{\beta}$C$H_2$–NH–).

### 2.2.2. Im-bzl-N,N′,N″-trihistidyl tris(2-aminoethyl)amine L3

Tris(2-aminoethyl)amine L1 (97 μl, 0.65 mmol) was added to an ice cold solution of dicyclohexylcarbodiimide (DCC) (0.44 g, 2.1 mmol), hydroxybenzotriazole (HOBt) (0.3 g, 1.95 mmol), and *N*((α)-*t*-butoxycarbonyl-*N*-(π)-benzyl-L-histidine (0.66 g, 1.95 mmol) in dimethylformamide (DMF) (8 ml) and the pH was adjusted to 7 using *N*-methyl morpholine (NMM). The reaction mixture was stirred at 0°C for 2 h and at room temperature for 12 h, filtered and evaporated to produce a solid which was suspended in $CH_2Cl_2$ (30 ml), extracted with 10% aqueous sodium carbonate (10 ml) and dried. The remaining solid was dissolved in EtOAc (5 ml) and kept at 4°C overnight. Dicyclohexylurea (DCU) was then filtered off and the solvent was evaporated to give a hygroscopic powder. $^1$H NMR ($CDCl_3$): 7.36 (s, 3H; im 2′), 7.28–7.21 (m, 9H; H-b, c), 7.10–7.05 (m, 6H; H-a), 6.65 (s, 3H; im 5′), 6.18 (br, s,3H; amide–NH), 4.95 (s, 6H; PhC$H_2$), 4.31–4.29 (m, 3H; His–$^{\gamma}$C*H*), 3.18–3.13 (m, 6H; –$^{\alpha}$C$H_2$), 2.81–2.78 (m, 6H; His–C$H_2$), 2.55–2.50 (m, 6H; –$^{\beta}$C$H_2$–), 1.34 (s, 27H, Boc); $C_{60}H_{81}N_{13}O_9$ (1128), FAB$^+$-MS: *m*/*z*: 1129 $[M+H]^+$.

Fully protected artificial trihistidine ((N(α)-Boc-im-bzl-L-His)$_3$tris(2-aminoethyl)-amine (0.35 g, 0.46 mmol) was dissolved in trifluoroacetic acid (TFA) and stirred for 0.5 h. Afterwards TFA was evaporated and the remaining solid was dissolved in water (10 ml) and washed using EtOAc (3 × 15 ml). The aqueous phase was dried up to give L3·7$CF_3COOH$ as a colorless solid product. Found: C, 41.95; H, 4.24; N, 10.94. *Anal*. Calc. for $C_{45}H_{57}N_{13}O_3$·7$CF_3COOH$·3$H_2O$: C, 42.19; H, 4.20; N, 10.84%. $^1$H NMR ($D_2O$): 8.72 (s, 3H; im 2′), 7.40–7.38 (m, 9H; H-b, c), 7.29–7.27 (m, 6H; H-a and 3H; im 5′), 5.27 (s, 6H; PhC$H_2$), 4.12 (t, 3H; His–$^{\gamma}$C*H*), 3.19 (d, 6H; $^{\alpha}$C$H_2$), 3.14–3.11 (m, 6H; His–C$H_2$), 3.09–3.00 (m, 6H; –$^{\beta}$C$H_2$–).

About 50 mg of L3·7$CF_3COOH$ passed through an anion exchange column (Dowex, $OH^-$ form) and the counteranion was changed from trifluoroacetate to $OH^-$. The eluted solvent of pH between 8 and 10 was collected, and water was evaporated; $^1$H NMR ($D_2O$): 7.63 (s, 3H; im 2′), 7.25–7.20 (m, 9H; H-b, c), 7.15–7.12(m, 6H; H-a), 6.81 (s, 3H; im 5′), 4.95 (s, 6H; PhC$H_2$), 4.03 (t, 3H; His–$^{\gamma}$C*H*), 3.00 (t, 6H; –$^{\alpha}$C$H_2$), 2.78 (d, 6 H; His–C$H_2$), 2.44–2.34 (m, 6H; –$^{\beta}$C$H_2$–); $C_{45}H_{57}N_{13}O_3$ (828), FAB-Mass: *m*/*z*: 829 $[M+H]^+$.

### 2.2.3. [L1ZnOH$_2$](ClO$_4$)$_2$ (1)

L1 (0.269 ml, 1.8 mmol) in methanol (10 ml) was added to a stoichiometric amount of Zn($ClO_4$)$_2$ (0.67 g, 1.8 mmol) in methanol (10 ml). The mixed solution was stirred for around 1 h. Single crystals suitable for X-ray crystallography of **1** were formed on standing for 1 week, separated, filtered off, washed with diethyl ether, and dried in vacuo. Found: C, 16.73; H, 4.45; Cl, 16.52; N, 12.98. *Anal*. Calc. For $C_6H_{20}Cl_2N_4O_9Zn$ ([L1ZnOH$_2$](ClO$_4$)$_2$): C, 16.81; H, 4.70; Cl, 16.54; N, 13.07%. $^1$H NMR ($D_2O$) 2.88 (t, 6H, –$^{\alpha}$C$H_2$) and 2.75 ppm (t, 6H, –$^{\beta}$C$H_2$–).

### 2.2.4. [L2ZnOH$_2$](ClO$_4$)$_2$ (2)

Complex **2** was prepared in a fashion similar to complex **1**. Found: C, 48.50; H, 5.51; Cl, 10.48; N, 8.27. *Anal*. Calc. For $C_{27}H_{35}Cl_2N_4O_9Zn$ ([L2ZnOH$_2$](ClO$_4$)$_2$): C, 48.49; H, 5.51; Cl, 10.47; N, 8.26%. $^1$HNMR ($D_2O$) 7.48–7.43 (m, 15H, –$C_6H_5$–), 3.34(s, 6H, Ph–C$H_2$–), 2.83 (t, 6H, –$^{\alpha}$C$H_2$) and 2.74 ppm (t, 6H, –$^{\beta}$C$H_2$–).

### 2.2.5. [HL3ZnOH$_2$](ClO$_4$)$_3$ (3)

Im-bzl-*N*,*N*′,*N*″-trihistidyl tris(2-aminoethyl)amine L3 (82 mg, 0.10 mmol) was dissolved in 2 ml MeOH/water (50%, v/v) and the pH was adjusted to 7 using 1 M $HNO_3$. Aqueous methanolic solution of Zn($ClO_4$)$_2$·6$H_2O$ (37 mg, 0.10 mmol) was then added. A white precipitate was produced, filtered off by membrane filter, washed out by ether, and dried up in vacuo. Found: C, 42.94; H, 4.70; Cl, 8.19; N, 14.78. *Anal*. Calc. for $C_{45}H_{60}Cl_3N_{13}O_{17}Zn$ ([HL3ZnOH$_2$](ClO$_4$)$_3$·$H_2O$): C, 43.93; H, 5.09; Cl, 8.66; N, 14.82%. $^1$H NMR ($D_2O$): 7.80 (s, 3H; im 2′), 7.30–7.24 (m, 9H; H-b, c), 7.20–7.17(m, 6H; H-a), 6.87 (s, 3H; im 5′), 4.99 (s, 6H; PhC$H_2$), 4.06 (t, 3H, His–$^{\gamma}$C*H*), 3.08 (t, 6H; –$^{\alpha}$C$H_2$), 2.88 (d, 6H; His–C$H_2$), 2.49–2.39 (m, 6H; –$^{\beta}$C$H_2$–).

### 2.2.6. [L1Zn–BNPP](ClO$_4$) (4)

Zinc complex **1** (0.428 g, 1 mmol) was dissolved in water (15 ml) at 40°C. bis(4-Nitrophenyl)phosphoric acid (HBNPP) (0.34 g, 1 mmol) was dissolved in water (15 ml). The solutions were combined and stirred for 24 h. The solvent was evaporated and dried in vacuo. Colorless crystals suitable for X-ray crystallography were grown by vapour diffusion of diethyl ether into a solution of the complex in methanol. Found; C, 33.31; H, 4.08; Cl, 5.39; N, 12.86. *Anal*. Calc. for $C_{18}H_{26}N_6O_{12}PClZn$: C, 33.25; H, 4.03; Cl, 5.45; N, 12.93%. $^1$H NMR ($D_2O$) 8.17–8.15 and 7.28–7.25 (m, 8H, –$C_6H_5$–), 2.75 (t, 6H, –$^{\alpha}$C$H_2$), and 2.63 ppm (t, 6H, –$^{\beta}$C$H_2$–). $^{31}$P NMR for **4** and free $BNPP^-$ in $D_2O$ (85% $H_3PO_4$ as external reference) showed −9.79 and −6.79 ppm, respectively.

## 2.3. Measurements

### 2.3.1. X-ray structure determination of 1 and 4

Zinc complexes **1** and **4** were isolated as colorless crystals to obtain structural information. X-ray mea-

Table 1
Crystal data and structure refinement of complexes $[L1Zn–OH_2]^{2+}$ (**1**) and $[L1Zn–BNPP]^{+}$ (**4**)

| Complex | **1** | **4** |
|---|---|---|
| Empirical formula | $C_6H_{20}N_4O_9Cl_2Zn$ | $C_{18}H_{26}N_6O_{12}PClZn$ |
| Formula weight (g $mol^{-1}$) | 428.53 | 650.24 |
| $T$ (K) | 123 | 123 |
| Crystal system | monoclinic | monoclinic |
| Crystal size (mm) | $0.40\times0.15\times0.10$ | $0.30\times0.10\times0.10$ |
| Space group | $Cc$ (no. 9) | $P2_1/c$ (no. 14) |
| Unit cell dimensions | | |
| $a$ (Å) | 16.264(1) | 8.291(1) |
| $b$ (Å) | 16.338(2) | 26.240(2) |
| $c$ (Å) | 23.216(3) | 11.269(1) |
| $\beta$ (°) | 95.80(1) | 93.08(1) |
| $V$ (Å$^3$) | 6137(1) | 2526.4(1) |
| $Z$ | 16 | 4 |
| $D_{calc}$ (g $cm^{-3}$) | 1.855 | 1.709 |
| $F(000)$ | 3520 | 1336 |
| $\mu$ (Mo/Cu Kα) ($cm^{-1}$) | 19.99 | 36.02 |
| Absorption coefficient ($cm^{-1}$) | 19.99 | 36.02 |
| $2\theta$ Range (°) | $3.5<2\theta<55$ | $7.6<2\theta<135.7$ |
| Min./max. absorption correction | 0.69/0.82 | 0.41/0.70 |
| No. independent reflections | 28628 | 19508 |
| Merging factor $R_{int}$ | 0.046 | 0.033 |
| Reflections observed | 6420 | 3959 |
| Variable parameters | 794 | 353 |
| Final $R$ indices $[I>2\sigma(I)]$ [a] | $R=0.032$, $R_w=0.04$ | $R=0.037$, $R_w=0.06$ |
| Goodness-of-fit on $F$ | 1.22 | 1.38 |
| Largest difference peak and hole (e Å$^{-3}$) | 0.88 and −0.55 | 0.38 and −1.08 |

[a] $R=\Sigma||F_o|-|F_c||/\Sigma|F_o|$ and $R_w=[\Sigma w(|F_o|-|F_c|)^2/\Sigma w F_o^2]^{1/2}$.

surements for complexes **1** and **4** were performed at 123 K on a Rigaku Imaging Plate diffractometer RAXIS–RAPID using graphite monochromated Mo Kα radiation ($\lambda=0.71069$ Å) for complex **1** and monochromated Cu Kα radiation ($\lambda=1.54178$ Å) for complex **4**. Data have been corrected for Lorentz and polarization effects. Crystal data and information on data collection are given in Table 1. The structures were solved by direct methods [12] and expanded using Fourier techniques [13]. Non-hydrogen atoms were refined anisotropically. Hydrogens were included but not refined. All calculations were carried out using the teXsan crystallographic software package developed by Molecular Structure Corporation (1985 and 1999).

### 2.3.2. Potentiometric measurements

Potentiometric titrations were carried out at 25 ± 0.2°C with a TOA AUT-501 automatic titrator connected to a TOA ABT-511 automatic buret with a combined glass electrode. The titrator cell was flushed with nitrogen gas during the experiments. The electrode was calibrated using standard aqueous buffers. Solutions were made up with aqueous methanol (33%, v/v) and the ionic strength was adjusted to 0.1 M by adding appropriate amounts of $NaNO_3$. To compensate for the methanol–water liquid junction potential, a correction of 0.136 pH units was substracted from the measured pH readings [14]. The solution of 1.00 mM L1, L2 (5 mM $HNO_3$) and L3 (9.00 mM $HNO_3$) in the absence (for determination of ligand deprotonation constants, $K_a$) and in the presence of equivalent $Zn^{2+}$ ion (for determination of stability constants $K_{st}$ and deprotonation constants $K_a$ of $Zn^{2+}$-bound $H_2O$) were titrated with 0.1 M NaOH aqueous solution, respectively. For the titrations, every increment of NaOH (50 μl) was added with an equilibration time of 60 s after each addition. Equilibrium constants were calculated using the program BEST [15] and species distributions were calculated using the program SPE [15].

### 2.3.3. $^1H$ NMR measurements

To confirm stoichiometry of zinc complexes **1**, **2** and **3**, $^1H$ NMR analyses of the nature of $L1/Zn^{2+}$, $L2/Zn^{2+}$ and $L3/Zn^{2+}$ binding were undertaken as a function of added $Zn^{2+}$. The concentration of the ligands ($2\times10^{-3}$ M) in aqueous methanol (33% $CD_3OD$, v/v, $I=0.1$ M $NaNO_3$) was kept constant at a pH of approximately 9 for L2 and a pH of approximately 7 for L3 at 30°C. Chemical shifts are reported relative to the resonance signal of sodium 2,2-dimethyl-2-silapentane-5-sulfonate (DSS) as internal standard. The p$D$ was adjusted with concentrated NaOD and $DNO_3$, so that the effect of dilution could be neglected.

### 2.3.4. Hydrolysis reaction of bis(4-nitrophenyl)phosphate (BNPP) and tris(4-nitrophenyl)phosphate (TNPP)

The hydrolysis rate of $BNPP^-$ and TNPP catalyzed by $Zn^{2+}$-bound hydroxo species of **1**, **2** and **3** in aqueous methanol (33% $CH_3OH$, v/v) was measured following an increase in 402 nm absorption of released $p$-nitrophenolate as a hydrolysis product. The pH of each sample was adjusted by using 1 M $NaOH/HNO_3$, and not by using buffers in order to avoid any catalytic or inhibition effect. In the course of hydrolysis, the pH of each sample was checked and was found that the difference compared to the adjusted pH value at the beginning of hydrolysis was not larger than 0.3.

For $BNPP^-$ hydrolysis the samples of 1 mM of **1**, **2** and **3** were incubated at 50°C, while the applied $BNPP^-$ concentration was 20 μM. All reactions showed first-order characteristics and were followed up to five half lives. Whereas the measurements of TNPP hydrolysis were carried out at 25 ± 0.2°C. Since further hydrolysis of the formed $BNPP^-$ is slower by several magnitudes, release of only one $p$-nitrophenolate per

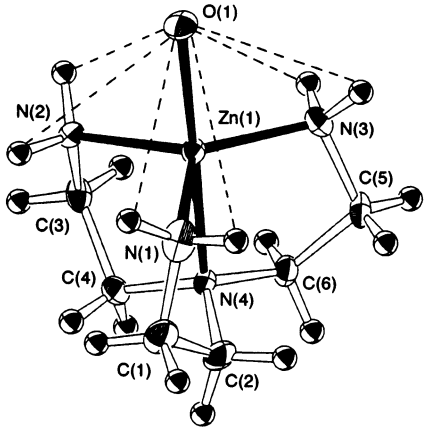


Fig. 1. ORTEP drawing of molecular structure of $[L1ZnOH_2]^{2+}$ (**1**). Ellipsoids are depicted at the 50% probability level. The intramolecular distances (dashed lines) are equal to around 3.0–3.4 Å.

TNPP molecule was considered. Reactions were initiated by rapid injection of tetrahydrofurane (THF) solution of 60 μl of 2.0 mM TNPP into 3 ml of 1.0 mM zinc complex solutions. The absorption increase was immediately monitored until $\geq 4t_{1/2}$. Reaction rates are corrected by blank experiments which were made up similarly but without the presence of the zinc complexes. The pseudo-first order rate constants, as before, were estimated from the integrated form of the first-order law.

## 3. Results and discussion

### *3.1. Description of the molecular structures of model complexes **1** and **4***

Figs. 1 and 2 show ORTEP drawings of the molecular structures of $[ZnL1(OH_2)]^{2+}$ (**1**) and $[ZnL1(BNPP)]^{+}$ (**4**) with 50% probability thermal elliposoids. Selected bond lengths and bond angles around the Zn(II) ion for both zinc-bound model complexes are given in Tables 2 and 3.

The molecular structure of $[L1Zn{-}H_2O]^{2+}$, shown in Fig. 1, has approximate $C_3$ symmetry: the zinc ion is surrounded by four nitrogens from L1 and one water molecule in a slightly distorted trigonal-bipyramidal configuration. The tertiary amine nitrogen N(4) and the water oxygen O(1) are located at the apices, and the three primary amine nitrogens (N(1), N(2) and N(3)) at the equatorial positions. The very weak axial Zn–N(4) interaction with bond distance of 2.193(4) Å is significantly longer than the equatorial Zn–N distances with an average of 2.051(5) Å. Similar values have been found in $[L1ZnNCS]^{+}$ [16]: 2.058(5) for the equatorial Zn–N distances and 2.292(4) Å for the apical Zn–N distance. The equatorial N–Zn–N angles are all with an average of 118.5(2)°. The intrachelate N–Zn–N(4) bond angles, all three of which are equal to the value of 83.07(2)°, differ from the value of 80.9° reported for $[L1ZnNCS]^{+}$. The Zn(1)–O(1) bond distance of 2.121(4) Å and the O(1)–Zn–N(4) angle of 175.5(2)°

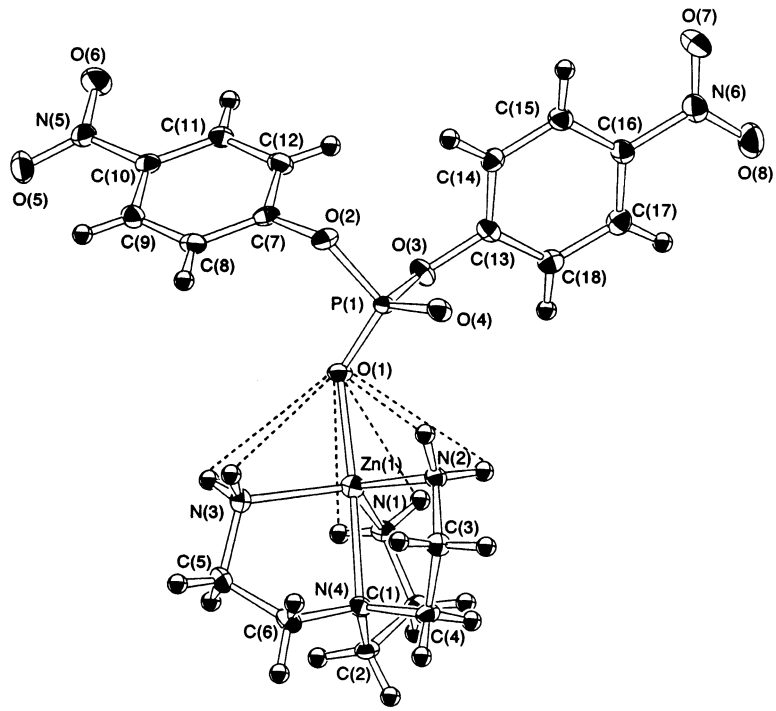


Fig. 2. ORTEP drawing of molecular structure of $[L1Zn{-}BNPP]^{+}$ (**4**). Ellipsoids are depicted at the 50% probability level. The intramolecular distances (dashed lines) are equal to around 3.0–3.4 Å.

Table 2
Selected bond lengths (Å) and bond angles (°) of $[L1Zn–OH_2]^{2+}$ (**1**)

| | | | |
|---|---|---|---|
| *Bond lengths* | | | |
| Zn(1)–O(1) | 2.121(4) | Zn(1)–N(1) | 2.070(5) |
| Zn(1)–N(2) | 2.039(5) | Zn(1)–N(3) | 2.044(5) |
| Zn(1)–N(4) | 2.193(4) | N(1)–C(1) | 1.472(7) |
| N(2)–C(3) | 1.466(8) | N(3)–C(5) | 1.485(8) |
| N(4)–C(2) | 1.478(7) | N(4)–C(4) | 1.465(7) |
| N(4)–C(6) | 1.476(7) | C(1)–C(2) | 1.520(8) |
| C(3)–C(4) | 1.528(8) | C(5)–C(6) | 1.524(9) |
| *Bond angles* | | | |
| O(1)–Zn(1)–N(1) | 95.2(2) | O(1)–Zn(1)–N(2) | 100.7(2) |
| O(1)–Zn(1)–N(3) | 95.0(2) | O(1)–Zn(1)–N(4) | 175.5(2) |
| N(1)–Zn(1)–N(2) | 115.9(2) | N(1)–Zn(1)–N(3) | 120.2(2) |
| N(1)–Zn(1)–N(4) | 82.3(2) | N(2)–Zn(1)–N(3) | 119.5(2) |
| N(2)–Zn(1)–N(4) | 83.7(2) | N(3)–Zn(1)–N(4) | 83.2(2) |
| Zn(1)–N(1)–C(1) | 108.5(3) | Zn(1)–N(2)–C(3) | 107.7(3) |
| Zn(1)–N(3)–C(5) | 109.6(4) | Zn(1)–N(4)–C(2) | 106.8(3) |
| Zn(1)–N(4)–C(4) | 105.1(3) | Zn(1)–N(4)–C(6) | 105.8(3) |
| C(2)–N(4)–C(4) | 112.6(4) | C(2)–N(4)–C(6) | 112.9(4) |
| C(4)–N(4)–C(6) | 113.0(4) | N(1)–C(1)–C(2) | 108.9(4) |
| N(4)–C(2)–C(1) | 110.2(4) | N(2)–C(3)–C(4) | 109.3(5) |
| N(4)–C(4)–C(3) | 109.8(5) | N(3)–C(5)–C(6) | 108.5(5) |
| N(4)–C(6)–C(5) | 111.5(5) | | |

Table 3
Selected bond lengths (Å) and bond angles (°) of $[L1Zn–BNPP]^{+}$ (**4**)

| | | | |
|---|---|---|---|
| *Bond lengths* | | | |
| Zn(1)–O(1) | 2.059(2) | Zn(1)–N(1) | 2.058(2) |
| Zn(1)–N(2) | 2.067(2) | Zn(1)–N(3) | 2.057(2) |
| Zn(1)–N(4) | 2.246(2) | P(1)–O(1) | 1.496(2) |
| P1(1)–O(2) | 1.611(2) | P(1)–O(3) | 1.616(2) |
| P1(1)–O(4) | 1.472(2) | O(2)–C(7) | 1.383(3) |
| O(3)–C(13) | 1.378(3) | O(5)–N(5) | 1.220(3) |
| O(6)–N(5) | 1.229(3) | O(7)–N(6) | 1.215(3) |
| O(8)–N(6) | 1.230(3) | N(1)–C(1) | 1.486(3) |
| N(2)–C(3) | 1.485(3) | N(3)–C(5) | 1.478(3) |
| N(4)–C(2) | 1.471(3) | N(4)–C(4) | 1.473(3) |
| N(4)–C(6) | 1.472(3) | N(5)–C(10) | 1.473(3) |
| N(6)–C(16) | 1.476(3) | | |
| *Bond angles* | | | |
| O(1)–Zn(1)–N(1) | 102.02(8) | O(1)–Zn(1)–N(2) | 98.84(8) |
| O(1)–Zn(1)–N(3) | 94.05(8) | O(1)–Zn(1)–N(4) | 175.36(7) |
| N(1)–Zn(1)–N(2) | 118.19(9) | N(1)–Zn(1)–N(3) | 115.21(9) |
| N(1)–Zn(1)–N(4) | 82.11(9) | N(2)–Zn(1)–N(3) | 120.47(9) |
| N(2)–Zn(1)–N(4) | 80.88(8) | N(3)–Zn(1)–N(4) | 82.19(8) |
| Zn(1)–O(1)–P(1) | 130.5(1) | O(1)–P(1)–O(2) | 108.7(2) |
| O(1)–P(1)–O(3) | 104.3(2) | O(1)–P(1)–O(4) | 121.6(1) |
| O(2)–P(1)–O(3) | 102.69(10) | O(2)–P(1)–O(4) | 106.7(1) |
| O(3)–P(1)–O(4) | 111.3(1) | P(1)–O(2)–C(7) | 122.7(2) |
| P(1)–O(3)–C(13) | 123.1(2) | Zn(1)–N(1)–C(1) | 109.8(1) |
| Zn(1)–N(2)–C(3) | 111.8(2) | Zn(1)–N(3)–C(5) | 111.6(2) |
| Zn(1)–N(4)–C(2) | 105.3(1) | Zn(1)–N(4)–C(4) | 106.9(2) |
| Zn(1)–N(4)–C(6) | 104.7(1) | C(2)–N(4)–C(4) | 112.5(2) |
| C(2)–N(4)–C(6) | 113.8(2) | C(4)–N(4)–C(6) | 112.7(2) |
| O(5)–N(5)–O(6) | 123.7(2) | O(5)–N(5)–C(10) | 118.6(2) |
| O(6)–N(5)–C(10) | 117.6(2) | O(7)–N(6)–O(8) | 124.2(2) |
| O(7)–N(6)–C(16) | 118.6(2) | O(8)–N(6)–C(16) | 117.2(2) |

which indicates some deviation from $C_3$ symmetry are within the values previously observed for other polyamine zinc complexes with oxygen coligands [17].

The molecular structure of $[L1Zn(BNPP)]^{+}$ is shown in Fig. 2. The essential part of **4** consists of Zn(II) ion, L1, and $BNPP^{-}$ anion. The zinc atom adopts the same slightly distorted trigonal-bipyramidal coordination geometry as has been described above for complex **1** with N(1), N(2), and N(3) of L1 on the basal plane and N(4) and O(1) of $BNPP^{-}$ at the apex. The axial Zn–N(4) interaction with bond distance of 2.246(2) Å is significantly longer than the equatorial Zn–N distances, which are in the range of 2.057(2)–2.067(2) Å. $BNPP^{-}$ acts as a monodentate ligand occupying the fifth site of the coordination sphere around Zn(II) in the *trans* position with respect to the four bridgehead nitrogens. The Zn–O(1) bond distance (2.059(2) Å) of phosphate ligand in **4** is shorter than Zn–O(1) bond distance (2.134(4) Å) of zinc-bound $H_2O$ in **1**, and is rather long compared with other related bonds [18]. Correspondingly the two P–O bonds which do not bear *p*-nitrophenyl substituents are of almost equal lengths (average 1.484 Å). This indicates that $BNPP^{-}$ ligand is still quite anionic and has a rather low degree of single bond location in the P–O–Zn unit.

Although great deal of efforts have been made to develop models as catalysts for phosphoester hydrolysis, crystal structures determined for zinc-containing catalysts are scarce. These with zinc-bound $H_2O$ molecule are especially few [7a,g,r]. The crystal structure determination of the complexes **1** and **4** showed the direct evidence for the presence of coordinated $H_2O$ molecule and binding of the substrate ($BNPP^{-}$), which play an essential role in the hydrolytic reaction mechanism.

### 3.2. Deprotonation and zinc complexation constants of L1, L2, and L3

These complexes **1**, **2** and **3** provided an opportunity to examine the effect of changing the environment on the $pK_a$ of the coordinated water molecule. Typical set of pH titration and species distribution curves for L2 and L3 in the absence and in the presence of stoichiometric amounts of $Zn^{2+}$ are shown in Figs. 3 and 4. The obtained deprotonation constants $pK_a$ are summarized in Table 4.

The $pK_a$ values for L1 in 33% $MeOH/H_2O$ showed no significant change compared to the previously reported values measured in purely aqueous medium [11a]. The decreased basicity of amino groups in L2 compared to L1 can be attributed to the electron withdrawing effect of benzyl groups attached to the amino moieties.

In ligand L3, seven consecutive deprotonation steps were observed. The first four deprotonation constants were assigned to the tertiary amine and the three imidazole nitrogens (Table 4). In dipeptides, where the amino

group of histidine is unprotected, the p$K_a$ of the imidazole nitrogens is lower than in histidine: e.g. 5.39 in His–Gly, 5.65 in His–Leu while this value is 5.87 in histidine [19]. In structurally similar peptides, *N*,*N*′-di-L-histidylethane-1,2-diamine (dhen), p$K_a$ values of 4.62 and 5.32 were reported for the imidazole nitrogens [20], while these values in another compound im-bzl *N*,*N*′-dihistidyldiethylenetriamine are 4.3 and 4.9 respectively [7u]. A tren-based tripodal imidazole containing ligand has more basic imidazole nitrogens [10a] because it lacks other aliphatic nitrogens which is found in L3. Consequently, in L3, the presence of these aliphatic amines makes the imidazol groups more acidic.

The potentiometric pH titration curve for ligands in the presence of equimolar $Zn^{2+}$ revealed complex formations until [OH]/[L] = 3 for L1 and L2 and = 7 for L3. But in all cases Zn complexes reacted with more $OH^-$ than what was needed to fully deprotonate the ligands. This means each complex contains one extra deprotonable group which is not present in the ligands themselves.

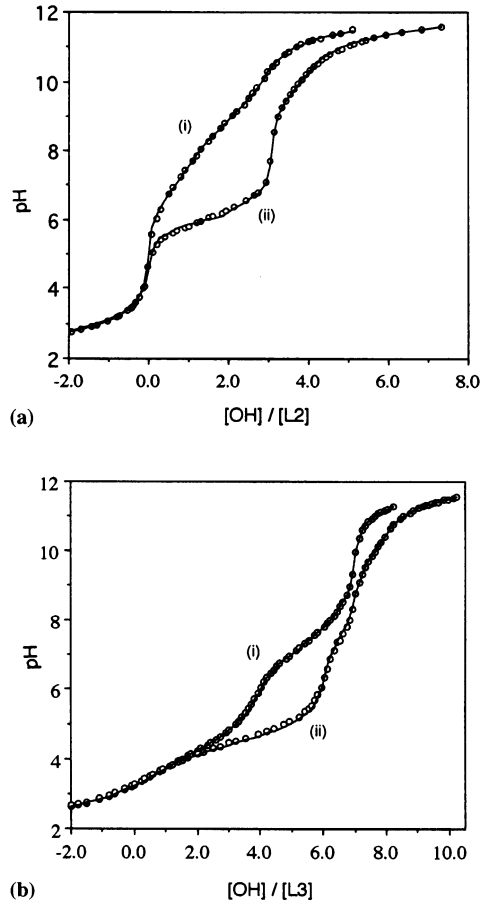


Fig. 3. (a) pH titration curves (○ observed, — calculated) of $1.0 \times 10^{-3}$ M L2 in the presence of $2.0 \times 10^{-3}$ M $HNO_3$ in aqueous MeOH (33%, v/v) at $I = 0.1$ M $NaNO_3$ and 25°C (i) in the absence of $Zn^{2+}$ and (ii) in the presence of equimolar amount of $Zn^{2+}$. (b) pH titration curves (○ observed, — calculated) of $1.0 \times 10^{-3}$ M L3 in the presence of $2.0 \times 10^{-3}$ M $HNO_3$ in aqueous MeOH (33%, v/v) at $I = 0.1$ M $NaNO_3$ and 25°C (i) in the absence of $Zn^{2+}$ and (ii) in the presence of equimolar amount of $Zn^{2+}$.

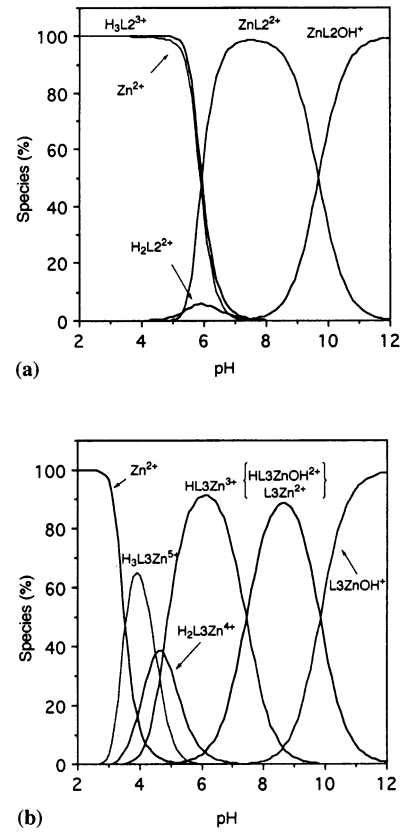


Fig. 4. (a) Species distribution curves of $1.0 \times 10^{-3}$ M L2 and $1.0 \times 10^{-3}$ M $Zn^{2+}$ in aqueous MeOH (33%, v/v) at $I = 0.1$ M $NaNO_3$ and 25°C. (b) Distribution curve of zinc-containing species of $1.0 \times 10^{-3}$ M L3 and $1.0 \times 10^{-3}$ M $Zn^{2+}$ in aqueous MeOH (33%, v/v) at $I = 0.1$ M $NaNO_3$ and 25°C.

Table 4
Deprotonation constants (p$K_a$) of L1, L2 and L3

| Species/reaction | | | | L1 | L2 | L3 |
|---|---|---|---|---|---|---|
| $HL^+$ | = | L | $+H^+$ | 10.47 | 9.46 | 7.94 |
| $H_2L^{2+}$ | = | $HL^+$ | $+H^+$ | 9.91 | 8.35 | 7.26 |
| $H_3L^{3+}$ | = | $H_2L^{2+}$ | $+H^+$ | 9.05 | 6.80 | 6.60 |
| $H_4L^{4+}$ | = | $H_3L^{3+}$ | $+H^+$ | | | 5.29 |
| $H_5L^{5+}$ | = | $H_4L^{4+}$ | $+H^+$ | | | 4.69 |
| $H_6L^{6+}$ | = | $H_5L^{5+}$ | $+H^+$ | | | 4.52 |
| $H_7L^{7+}$ | = | $H_6L^{6+}$ | $+H^+$ | | | 3.37 |

In the case of complexes **1** and **2**, the extra deprotonation can only be assigned to the deprotonation of water molecule ligated to the central zinc ion of the complexes.

In the case of complex **3**, the extra deprotonation could be assigned to two different processes: (i) deprotonation of the coordinated water molecule; or (ii) metal-promoted deprotonation of the amide. Rabenstein et al. [21] showed that zinc(II)-promoted deprotonation of amide nitrogens in imidazole-containing

peptides generally results in kinetically stable complexes. The chemical shifts of the protons near to the amide nitrogen are considerably altered. In order to clarify whether the amide nitrogens are coordinated to zinc or not, we have conducted $^1$H NMR titration measurements for ligand L3 ($2 \times 10^{-3}$ M) in the presence of equimolar amount of $Zn^{2+}$ ion in 33% $CD_3OD$–$D_2O$ as a function of p*D* (above p*D* 6). Through this, we found out that the methylene protons of the tren part ($\beta$), directly linked to the amide nitrogens were weakly influenced (0.03 ppm). The above result strongly indicates that the extra deprotonation is only related to the formation of zinc-bound hydroxo species and not with metal-promoted deprotonation of amide nitrogens.

The obtained stability constants log$K_{st}$ and deprotonation constants p$K_a$ ($H_2O$) of zinc complexes are listed in Table 5. The potentiometric data indicated that L1 forms a much more stable complex with Zn(II) ($\log K_{st} = 15.05$) than does L2 ($\log K_{st} = 10.02$). The lowering in $\log K_{st}$ value of **2** compared to **1** is accompanied by the lowering in p$K_a$ for all secondary amino groups in L2. The p$K_a$($H_2O$) variation among **1** (10.72), 2 (9.61), and **3** (7.43) may arise because of different environments around each coordinated water molecule.

In the case of L3, titrimetrically detected complexes with different protonation states can exist as a function of pH. The low $\log K_{st}$ for $H_3L3Zn^{5+}$ is consistent with related complexes bearing only three imidazole donor functions [10a]. *N*-alkylation of the pyrrolic nitrogen in imidazole units reduces the metal binding ability of the ligand. For example in the case of tripodal *N*-methyl imidazole derivatives, $\log K_{st}$ decreases about three to four units, with a $\log K_{st}$ value of around 4, which is consistent with the analogous value of $HL3Zn^{3+}$ species [22]. Subsequent deprotonation of aliphatic amino groups forms complexes with increasing $\log K_{st}$ values indicating some contribution of amino nitrogens in coordination with the central zinc ion.

The monoprotonated complex species, $HL3ZnH_2O^{3+}$ contains zinc-bound water molecule and one protonated primary amino group. The proton loss of this species can occur either at the amino function to form $L3ZnH_2O^{2+}$ ($pK_a = 7.94$) or at the coordinated water molecule to form $HL3ZnOH^{2+}$ ($pK_a = 7.43$). As these species are titrimetrically equivalent, it is not possible to distinguish between them by pH–metric titration. Since the stability of {$HL3ZnOH^{2+}$/$L3ZnH_2O^{2+}$} is not much higher compared to $HL3ZnH_2O^{3+}$, it indicates that {$HL3ZnOH^{2+}$/$L3ZnH_2O^{2+}$} contains no new coordination site in comparison with $HL3ZnH_2O^{3+}$. A possible newly formed binding site would probably contribute to ligate the central zinc, resulting in higher log $K_{st}$ values. If the $HL3ZnOH^{2+}$ is formed, there is no increase in the coordination number of the central zinc and is not associated with dramatic change in $\log K_{st}$. From the above reasons we assume that when $HL3ZnH_2O^{3+}$ loses a single proton, the zinc-bound hydroxo species, rather than the $L3ZnH_2O^{2+}$ is formed.

Nevertheless, the primary amino function lies away from the cavity stabilized/fixed by the imidazolyl nitrogens. This means that even if the amino groups are deprotonated in the complex, it is difficult for these functionalities to bind the zinc center. If the deprotonation step involves formation of a free amino group, the $\log K_{st}$ value will not significantly increase compared to the protonated form. So the possibility that the proton loss of $HL3ZnOH_2^{3+}$ occurs in the amino functionality can not be completely excluded. When considering 2:1 ligand–Zn complex species, pH–titration curve analysis resulted in a worse fit. This is consistent with our previous assumption that the introduction of benzyl groups to each histidine side chain can prevent the formation of octahedral (2:1) complexes [7u].

Table 5
Stability constants ($\log K_{st}$), and deprotonation constants (p$K_a$) of the indicated species

| Species/reaction | | | | L1 | L2 | L3 |
|---|---|---|---|---|---|---|
| | | | | *log $K_{st}$* | | |
| $H_3L^{3+} + Zn^{2+}$ | = | $H_3LZn^{5+}$ | | | | 3.62 |
| $H_2L^{2+} + Zn^{2+}$ | = | $H_2LZn^{4+}$ | | | | 4.94 |
| $HL^{+} + Zn^{2+}$ | = | $HLZn^{3+}$ | | | | 8.38 |
| $L + Zn^{2+}$ | = | $LZn^{2+}$ | | 15.05 | 10.02 | 9.43 |
| | | | | *p$K_a$* | | |
| $HLZnOH_2^{3+}$ | = | $HLZnOH^{2}$ $LZnOH_2^{2+}$ | $+H^{+}$ | | | 7.43 |
| $HLZnOH^{2+}$ $LZnOH_2^{2+}$ | = | $LZnOH^{+}$ | $+H^{+}$ | | | 9.82 |
| $HLZnOH_2^{2+}$ | = | $LZnOH^{+}$ | $+H^{+}$ | 10.72 | 9.61 | |

### 3.3. $^1$H NMR titration

As shown in Fig. 5(a), when $R$ ($= [Zn^{2+}]_o/[L2]_o$) is between 0 and 1, the methylene protons (α and β) of L2 were separated into free and complexed signals which then shifted downfield to around $R = 0.8$. At $R = 1.0$, the free signals disappeared and only the complexed peaks were observed. Further addition of zinc did not cause any change in the spectra indicating full complexation. Conclusively, only 1:1 complex is formed under these conditions. Similar results for L1 with $Zn^{2+}$ was obtained by $^1$H NMR and pH–metric titrations confirmed the 1:1 stoichiometry [11a].

$^1$H NMR titration of L3 with $Zn^{2+}$ was performed as described for L2 (Fig. 5(b)). When $R$ ($= [Zn^{2+}]_o/[L3]_o$) is 0.4, extensive broadening of the imidazole

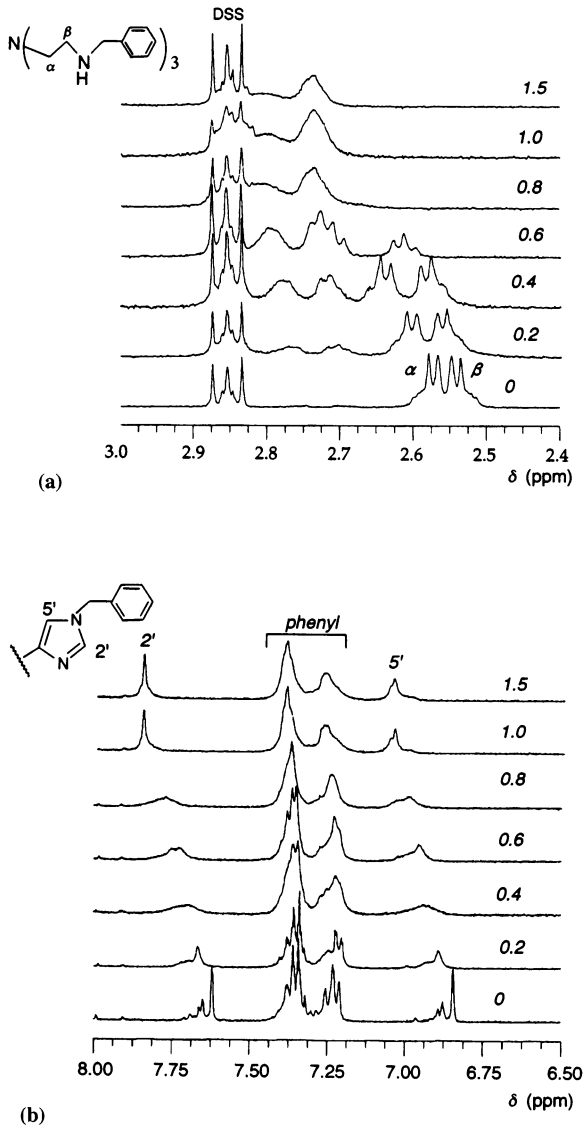


Fig. 5. (a) $^1$H NMR titration of L2 as a function of R ( $=[Zn^{2+}]_o/[L2]_o$) in aqueous MeOH-$d_4$ (33%, v/v) at $2.0\times10^{-3}$ M L2, $I=0.1$ M $NaNO_3$, pH 9 and 30°C; methylene (N–C$H_2$–C$H_2$–NH–) peaks are labelled α and β. (b) $^1$H NMR titration of L3 as a function of R ( $=[Zn^{2+}]_o/[L3]_o$) in aqueous MeOH-$d_4$ (33%, v/v) at $2.0\times10^{-3}$ M L3, $I=0.1$ M $NaNO_3$, pH 7 and 30°C; imidazole (–C$^2$H– and –C$^5$H–) peaks are labelled 2′ and 5′).

protons (2′ and 5′) signals indicated rapid ligand exchange. The effect of chemical exchange on the observed profiles gave coalescence between free and complexed signals. After 1 equiv. $Zn^{2+}$ was added, well resolved peaks of imidazole protons were observed which did not change when $R$ was increased to 1.5. Similarly to L1 and L2, all signals shifted downfield between $R=0$ and 1 but no further shift was observed at $R>1$. In contrast to L1 and L2 which contain only aliphatic donor groups, no separation between the complexed and free signals was found for L3. This phenomenon may be related to the differences in ligand exchange rates between **3** and the other two complexes **1** and **2**. The kinetic lability of $ZnL3^{2+}$ demonstrates the higher flexibility of the molecule and a better organized coordination environment around zinc ion. That explains why the peaks at $R>1$ are not completely sharpened which can also be a consequence of the lower log $K_{st}$ compared to **1** and **2**. Because of the rapid exchange processes of protons, zinc complex species with different protonation states gave averaged peaks which prevented us to characterize them separately.

### 3.4. Hydrolysis of activated esters by complexes *1*, *2* and *3*

The pH-dependence of the observed pseudo-first-order rate constants $k_{obsd}$ studied over a pH range of 6.5–11.0 for the hydrolysis of $BNPP^-$ and TNPP by using **1**, **2** and **3** are shown in Fig. 6(a) and (b). Higher rates were observed for the hydrolysis reaction of neutral phosphotriester TNPP compared to the single-negatively charged diester $BNPP^-$ because of the lack of

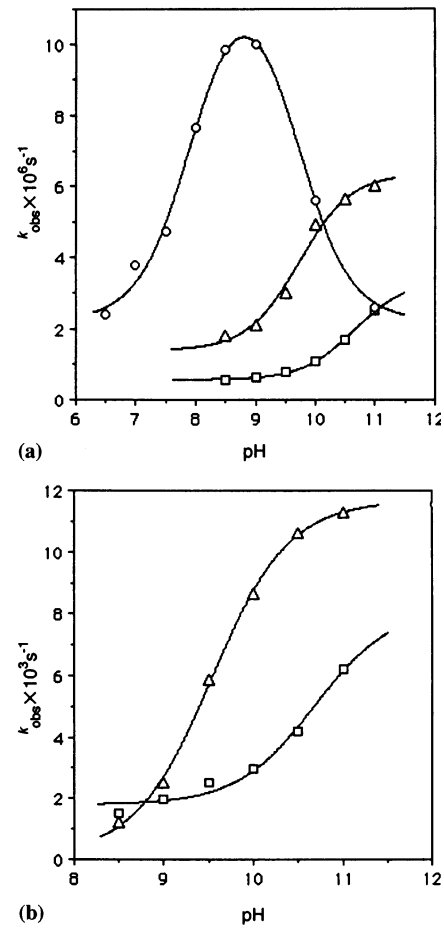


Fig. 6. Plots of the hydrolysis rate constant, $k_{obs}$ of (a) $2.0\times10^{-5}$ M BNPP and (b) $2.0\times10^{-5}$ M TNPP catalyzed by $1.0\times10^{-3}$ M Zn(II) complexes of **1** (□), **2** (△) and **3** (○) ($1.0\times10^{-3}$ M) at various pH values in water containing 33% MeOH by volume.

ionic repulsion between the nucleophilic zinc-bound hydroxide species and the substrate molecule, TNPP.

The pH–rate constant $k_{obsd}$ profiles for the hydrolysis of $BNPP^-$ (Fig. 6(a)) displayed sigmoidal curves for the catalytic reaction by **1** and **2**, while the pH–$k_{obsd}$ profile by **3** showed bell shape curve with inflexion points around the p$K_a$ values of the complexes.

The pH–rate constant $k_{obsd}$ profiles for the hydrolysis of TNPP (Fig. 6(b)) displayed sigmoidal curves for the catalytic reaction by the hydroxo species of **1** and **2**, while by **3** was too fast to be followed spectrophotometrically, the *p*-nitrophenolate immediately formed and its amount remained constant even after 5 days.

The p$K_a$ values obtained from these inflexion points are in good agreement with the p$K_a$ values determined by pH titration. Therefore, the zinc-bound hydroxo species of these complexes are believed to be active catalysts for hydrolyzing $BNPP^-$ and TNPP. The higher efficiency of **3** is in accordance with the decreased p$K_a(H_2O)$ value compared to that of **1** and **2**. Such pH profiles were observed in a number of phosphate ester hydrolyses promoted by $Zn^{II}$, $Co^{II}$, and $Cu^{II}$ complexes [23], and are indicative of the involvement of metal–hydroxo species. In our case, **1** and **2** possibly follow a common mechanism namely, the attack of the Zn–OH–nucleophile to the phosphorus center of the substrate, followed by the formation of intermediate containing pentacoordinated phosphorus, and release of *p*-nitrophenolate.

The rates of **1** catalyzed hydrolysis of $BNPP^-$ are consistent with previously reported values [24]. DeRosch and Trogler [24], found that the activity of complex **1** was comparable to the background blank system made by using buffers, so the effect of **1** was thought to be negligible. In contrast, we observed that the activity is attributed only to the complex. The pH of the reference solutions were adjusted by 1 M NaOH or $HNO_3$ and no hydrolysis was found even after two weeks in 33% MeOH. We have also tested the effect of solvent composition on the hydrolysis rates. Studies for the hydrolysis of $BNPP^-$ in purely aqueous medium by using **1** gave almost the same rate constants ($\pm$ 5%) compared with what was measured for samples made up with 33% methanol. In contrast with buffer, the solvent composition seems to have no effect on the catalytic activity.

The hydrolysis reaction by **3** was particularly fast compared to **1** and **2**: the observed rate constants $k_{obsd}$ for the release of *p*-nitrophenolate at pH 8.5 are $1.0 \times 10^{-5}$ $s^{-1}$ for **3**, $1.8 \times 10^{-6}$ $s^{-1}$ for **2**, and $5.5 \times 10^{-7}$ $s^{-1}$ for **1**, respectively. This large difference in rate enhancement may be attributed in part to the higher nucleophilicity of the metal-bound hydroxo species. Another major factor that contributes to the lower activity of **1** and **2** is their inhibition by the phosphodiester substrate as was confirmed by X-ray structure of L1Zn-bound BNPP (**4**). The crystal structure shows there is no other axial ligand than $BNPP^-$. This means that $BNPP^-$ acts as inhibitor and there is no nucleophile, which can intramolecularly attack $BNPP^-$. Because of this, we have conducted our kinetic studies by using excess of zinc complexes (catalysts) over the substrates.

These kinetically determined p$K_a$ values show high correlation for pH-metrically determined p$K_a$ of these complexes, namely $L1ZnH_2O^{2+} = L1ZnOH^+ + H^+$ for **1**, $L2ZnH_2O^{2+} = L2ZnOH^+ + H^+$ for **2** and $HL3ZnH_2O^{3+} = \{HL3ZnOH^{2+}/L3ZnH_2O^{2+}\} + H^+$ for **3**. In other words, the bell-shape pH-rate profile in the case of **3** largely correlates with the distribution curve (Fig. 4(b)) and provides strong evidence that this may be the catalytically active species in the hydrolysis.

As discussed before, by investigating the stability and deprotonation constants, there exists two species in solution in the pH range 6–11. The species of $\{HL3ZnOH^{2+}/L3ZnOH_2^{2+}\}$ was found to have maximum abundance around pH 8.5, wherein one is zinc-bound water and another is zinc-bound hydroxo species and terminal $NH_2$ groups exist as $NH_2/NH_3^+$ form. If the composition of this species was the tautomeric structure $L3ZnH_2O^{2+}$ alone, the metal-bound water would not be an appropriately strong nucleophile in the hydrolytic mechanism. Hence, no zinc complexes with coordinated water (being the exclusive active species) could perform that significant catalytic activity in cleaving the phosphoester bond in $BNPP^-$. So these two species may play a crucial role in the hydrolysis of $BNPP^-$, where easily exchangable water substituted by $BNPP^-$ and $OH^-$ acts as a nucleophile for the acceleration of hydrolysis reaction. From the p$K_a$ values of L3, $HL3^+$ species exists around pH 7.9 and above pH 8 this species gradually decreases, i.e. the $HL3ZnOH^{2+}$ also decreases. Around pH 10.5 $L3ZnOH^{2+}$ exists in solution, while zinc-bound water complex is absent. A question then arises as to why $L3ZnOH^+$ is practically inactive in this process. A probable explanation can come from the coordination properties of this species. Since the proton loss step of $HL3ZnOH^{2+}$ occurs in one of the primary amino function, the fully deprotonated complex contains one more ligation site compared to $HL3ZnOH^{2+}$ which may also coordinate to zinc. A possible increase in coordination number of zinc may radically change the conformation of the complex thus making it difficult for $OH^-$ to interact with the substrate. The hydrophobic benzyl groups attached to the imidazole binding sites can serve as hydrophobic microenvironment but due to their bulkiness, can also sterically hinder the approach of the substrate.

The surprisingly low p$K_a$ of the coordinated water molecule in 3 is about the range of the mononuclear zinc complexes found to be the most active [7g] and

almost the same value being reported for the hydrolytic $Zn^{2+}$-enzymes. The zinc complex of **3** is an artificial peptide–zinc complex, since the histidine side chains are attached to the tripodal amine, tren, via amide bond formation. Thus, this formation keeps zinc as a natural ion in the complex. The peptide zinc complexes which structurally and functionally mimic the active sites of phosphatase enzyme are very rare.

Attaching different side chains to L1 to form L2 and L3 had completely different effects on the coordination properties with zinc ion. The hydrophobic pocket in L3 is provided by the tren moiety centered by the tertiary nitrogen. The three histidyl residues coupled to tren mimicked the histidine side chain in large proteins, which is common in the active site of several zinc enzymes. We tried to attach benzyl groups to each histidyl unit in order to: (i) increase the hydrophobicity around zinc; (ii) avoid octahedral dimer formation by introducing benzyl groups as a steric hindrance; and (iii) help binding of aromatic substrates by $\pi-\pi$ stacking. The reason why L3 is more advantageous in comparison to L2 can be summarized in the following statements: (i) the donation sites of imidazoles have kinetically more labile binding ability; (ii) there is a larger spacer distance between the imidazole donor set and the tertiary nitrogen; (iii) there is an increased flexibility for coordination thus forming a more optimal geometry; and (iv) for steric reasons, it is impossible to bind the central tertiary nitrogen.

## 4. Supplementary material

Crystal data for complexes **1** and **4** are available from the author (KI, ichikawa@ees.hokudai.ac.jp) on request.

## References


[1] B.L. Vallee, A. Galdes, Adv. Enzymol. 56 (1984) 283.

[2] J.E. Coleman, Zinc Enzymes, Birkhauser, Boston, MA, 1986, p. 49.

[3] E.E. Kim, H.W. Wyckoff, J. Mol. Biol. 218 (1991) 449.

[4] J.E. Coleman, J.F. Chlebowski, Adv. Inorg. Biochem. 1 (1979) 2.

[5] A. Vedani, D.W. Huhta, S.P. Jaober, J. Am. Chem. Soc. 111 (1989) 4075.

[6] (a) R.H. Prince, P.R. Woolley, Angew. Chem., Int. Ed. Engl. 11 (1972) 408. (b) H. Coates, G.J. Gentle, S.F. Lincoln, Nature 249 (1974) 773.

[7] (a) P. Woolley, Nature 258 (1975) 677. (b) H. Slebocka-Tilk, J.L. Cocho, Z. Frakman, R.S. Brown, J. Am. Chem. Soc. 106 (1984) 2421. (c) J. Chin, X. Zou, J. Am. Chem. Soc. 106 (1984) 3687. (d) S.H. Gellman, R. Petter, R. Breslow. J. Am. Chem. Soc. 108 (1986) 2388. (e) P.R. Norman, A. Tate, P. Rich, Inorg. Chim. Acta 145 (1988) 211. (f) R.G. Clewley, H. Slebocka-Tilk, R.S. Brown, Inorg. Chim. Acta 157 (1989) 233. (g) E. Kimura, T. Shiota, T. Koike, M. Shiro, M. Kodama, J. Am. Chem. Soc. 112 (1990) 5805. (h) R. Alsfasser, S. Trofimenko, A. Looney, G. Parkin, H. Vahrenkamp, Inorg. Chem. 30 (1991) 4098. (i) T. Koike, E. Kimura, J. Am. Chem. Soc. 113 (1991) 8935. (j) N. Kitajima, S. Hikichi, M. Tanaka, Y. Moro-oka, J. Am. Chem. Soc. 115 (1993) 5496. (k) X. Zhang, R. Van Eldik, T. Koike, E. Kimura, Inorg. Chem. 32 (1993) 5749. (l) A. Looney, R. Han, K. McNeill, G. Parkin, J. Am. Chem. Soc. 115 (1993) 4690. (m) E. Kimura, I. Nakamura, T. Koike, M. Shionoya, Y. Kodama, T. Ikeda, M. Shiro, J. Am. Chem. Soc. 116 (1994) 4764. (n) H. Adams, N.A. Bailey, D.E. Fenton, Q.-Yu. He, J. Chem. Soc., Dalton Trans. (1995) 697. (o) T. Tanase, J.W. Yun, S.J. Lippard, Inorg. Chem. 35 (1996) 3585. (p) K. Nakata, M.K. Uddin, K. Ogawa, K. Ichikawa, Chem. Lett. (1997) 991. (q) J. Suh, S.J. Son, M.P. Suh, Inorg. Chem. 37 (1998) 4872. (r) K. Ogawa, K. Nakata, K. Ichikawa, Chem. Lett. (1998) 797. (s) P.E. Jurek, A.E. Martell, Inorg. Chem. 38 (1999) 6003. (t) P.E. Jurek, A.E. Martell, Inorg. Chim. Acta 287 (1999) 47. (u) K. Ichikawa, M.K. Uddin, K. Nakata, Chem. Lett. (1999) 115. (v) H. Kurosaki, T. Tawada, S. Kawasoe, Y. Ohashi, M. Goto, Bioorg. Med. Chem. Lett. 10 (2000) 1333. (w) T. Gajda, R. Kramer, A. Jancso, Eur. J. Inorg. Chem. (2000) 1635.

[8] A. Neuberger, K. Brocklehurst (Eds.), Hydrolytic Enzymes, Elsevier, Amsterdam, 1987.

[9] (a) P. Woolley, J. Chem. Soc., Perkin Trans. 2 (1977) 318. (b) R.S. Brown, M. Zamkanei, J.L. Cocho, J. Am. Chem. Soc. 106 (1984) 5222. (c) G.J.V. Driel, W.L. Driessen, J. Reedijk, Inorg. Chem. 24 (1985) 2919. (d) J. Chin, M. Banaszczyk, J. Am. Chem. Soc. 111 (1989) 2724. (e) R.W. Hay, A.K. Basak, M.P. Pujari, J. Chem. Soc., Dalton Trans. (1989) 197. (f) L. Iverson, R.A. Lerner, Science 243 (1989) 1185. (g) A. Abufarag, H. Vahrenkamp, Inorg. Chem. 34 (1995) 3279. (h) M.J. Young, D. Wahnon, R.C. Hynes, J. Chin, J. Am. Chem. Soc. 117 (1995) 9441. (i) P. Tecilla, U. Tonellato, A. Veronese, J. Org. Chem. 62 (1997) 7621. (j) M. Rombach, C. Maurer, K. Weis, E. Keller, H. Vahrenkamp, Chem. Eur. J. 5 (1999) 1013.

[10] (a) R. Jairam, P.G. Potvin, S. Balsky, J. Chem. Soc., Perkin Trans. 2 (1999) 363. (b) U. Herry, W. Spahl, G. Trojandt, W. Steglich, F. Thaler, R. Van Eldik, Biorg. Med. Chem. 7 (1999) 699.

[11] (a) J.W. Canary, J. Xu, J.M. Castagnetto, D. Rentzeperis, L.A. Marky, J. Am. Chem. Soc. 117 (1995) 11545. (b) X. Xu, A.R. Lajmi, J.W. Canary, J. Chem. Soc., Chem. Commun. (1998) 2701.

[12] A. Altomare, M.C. Burla, M. Camalli, G.L. Cascarano, C. Giacovazzo, A. Guagliardi, A.G.G. Moliterni, G. Polidori, R. Spagna, J. Appl. Crystallogr. 32 (1990) 115.

[13] P.T. Beurskens, G. Admiraal, G. Beurskens, W.P. Bosman, R. de Gelder, R. Israel, J.M.M. Smits, The DIRDIF-94 program system, Technical Report of the Crystallography Laboratory, University of Nijmegen, The Netherlands, 1994.

[14] R.G. Bates, M. Paabo, R.A. Robinson, J. Phys. Chem. 67 (1963) 1833.

[15] E.A. Martell, R.J. Motekaitis, The Determination and Use of Stability Constants, 2nd edn., VCH, New York, 1992, p. 143.

[16] G.D. Andreetti, P.C. Jain, J. Lingafelter, J. Am. Chem. Soc. 91 (1969) 411.

[17] (a) T. Brandsch, F. Schell, K. Weis, M. Ruf, B. Muller, H. Vahrenkamp, Chem. Ber./Recueil 130 (1997) 283. (b) M. Kato, T. Itoh, Inorg. Chem. 24 (1985) 509.

[18] S. Hikichi, M. Tanaka, Y. Moro-oka, N. Kitajima, J. Chem. Soc., Chem. Commun. (1992) 814.

[19] (a) M.J.A. Rainer, B.M. Rode, Inorg. Chim. Acta 93 (1984) 109. (b) R.P. Agarwal, D.D. Perrin, J. Chem. Soc., Dalton Trans. (1975) 1045.

[20] I. Torok, T. Gajda, B. Gyurcsik, G.K. Toth, A. Peter, J. Chem. Soc., Dalton Trans. (1998) 1205.

[21] D.L. Rabenstein, S.A. Daignault, A.A. Isab, A.P. Arnold, M.M. Shoukry, J. Am. Chem. Soc. 107 (1985) 6435.

[22] R.S. Brown, J. Huguet, Can. J. Chem. 58 (1980) 889.
[23] (a) J.R. Morrow, W.C. Trogler, Inorg. Chem. 27 (1988) 3387. (b) G.H. Raivji, R. Milburn, Inorg. Chim. Acta 150 (1989) 227. (c) J.R. Morrow, W.C. Trogler, Inorg. Chem. 28 (1989) 2330. (d) J. Burstyn, K.A. Deal, Inorg. Chem. 32 (1993) 3585. (e) W.H. Chapman, R. Breslow, J. Am. Chem. Soc. 117 (1995) 5462. (f) R.W. Hay, N. Govan, K.E. Parchment, Inorg. Chem. Commun. 1 (1998) 228.
[24] M.A. DeRosch, W.C. Trogler, Inorg. Chem. 29 (1990) 2409.